



OPTIMIZATION AND CHARACTERIZATION OF AZELAIC ACID NANOEMULSION FOR ENHANCED TOPICAL DELIVERY: A POTENTIAL THERAPEUTIC APPROACH FOR SKIN HYPERPIGMENTATION DISORDERS

Rahisuddin^{1*}, Nasiruddin Ahmad Farooqui², Dinesh Kumar Sharma³,

^{1*}Research Scholar, Sanskriti University, Mathura-Delhi Highway, Chhata, Mathura, 281401, U.P., India

²Professor, Translam Institute of Pharmaceutical Education and Research, Meerut, 250001, U.P., India

³Professor, Sanskriti University, Mathura-Delhi Highway, Chhata, Mathura, 281401, U.P., India

*Corresponding Author: Rahisuddin

Email ID: raiselder@yahoo.in

ABSTRACT:

This research focuses on the development and characterization of an Azelaic Acid nanoemulsion for improved topical delivery, targeting skin hyperpigmentation disorders. Using rapid connectivity homogenization and ultra-probe sonication, the nanoemulsion was optimized through Response Surface Methodology. Characterization involved various parameters, confirming successful encapsulation of Azelaic Acid. The optimized formulation exhibited favorable properties, including small globule size, high entrapment efficiency, and sustained release. Stability tests and ex-vivo permeation studies further supported its potential as a promising platform for treating skin hyperpigmentation disorders. Further research, including in vivo studies, is warranted for comprehensive efficacy and safety evaluation.

1. INTRODOCTION:

1.1 Structure of the skin

The skin is the largest organ of the human body and serves as a protective barrier between the internal organs and the external environment. It has several layers, each with distinct functions. The skin, serving as the body's primary interface with the external environment, ranks among the largest organs, encompassing an average area of 1.5 to 2.0 square meters and boasting a thickness of 1 to 2 millimeters. Its vital role unfolds across three key functions: safeguarding against mechanical trauma, UV radiation, microorganisms, and infections; overseeing regulation in terms of temperature, fluid balance, immunity, and vitamin D synthesis; and facilitating sensory experiences such as pressure, pain, heat, and cold [1].

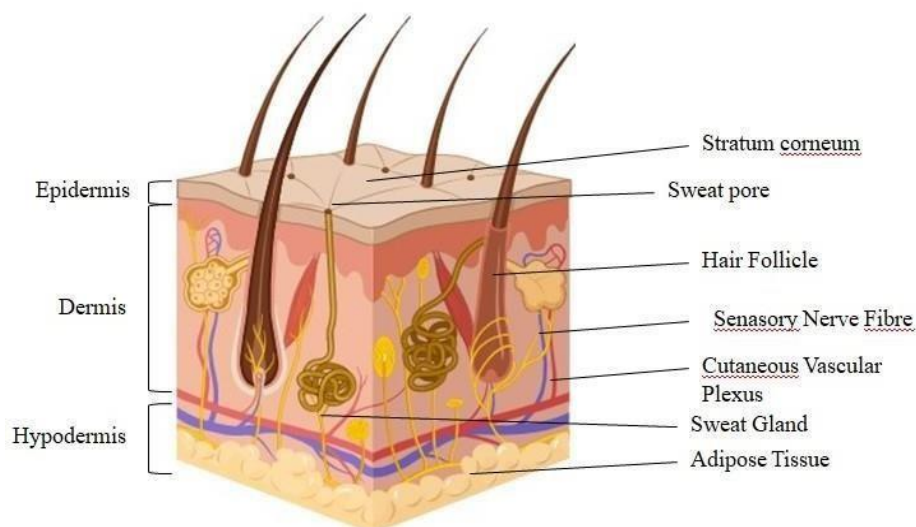


Figure 1. Structure of the skin

The initiation of melanogenesis involves the oxidation of L-tyrosine to dopaquinone, a critical step facilitated by the enzyme tyrosinase. This step is considered rate-limiting in melanin synthesis, as subsequent reactions can spontaneously proceed at physiological pH values. Dopaquinone, once generated, leucodopachrome is produced via intramolecular cyclization. Leucodopachrome and dopaquinone undergo a redox transfer that yields dopachrome and L-3,4-dihydroxyphenylalanine (L-dopa). Tyrosinase uses L-Dopa as a substrate, and when it oxidizes back into dopaquinone, an important enzymatic cycle is closed. The catalytic action of tyrosinase-related protein-2 (TRP-2), also known as dopachrome tautomerase (DCT), leads to the rearrangement of dopachrome, ultimately yielding 5,6-dihydroxyindole (DHI) and 5,6-dihydroxyindole-2-carboxylic acid (DHICA). These compounds serve as precursors for the final oxidation to melanin pigments. It has been suggested that tyrosinase-related protein-1 (TRP-1) catalyzes the conversion of DHICA to pigment. Importantly, the presence or absence of cysteine plays a determining role in the formation of pheomelanin (yellow/red pigment) or eumelanin (brown/black pigment) [30]. Despite the involvement of all three enzymes -tyrosinase, TRP-1, and TRP-2 in the melanogenesis pathway, tyrosinase is exclusively indispensable for the overall melanin production process [2].

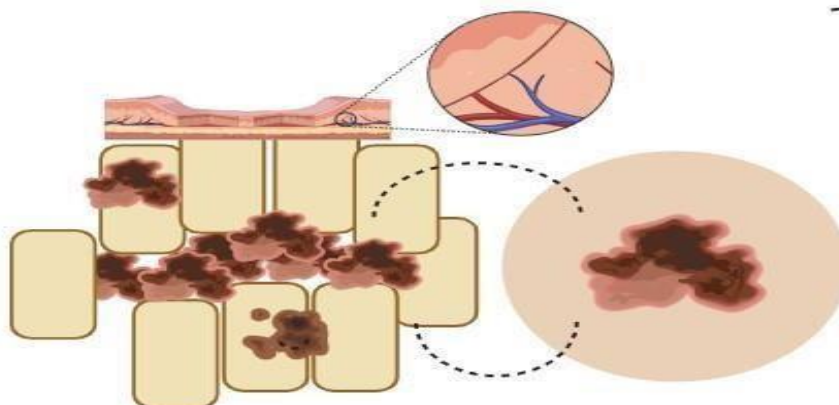


Figure 2: Schematic representation of Melanin transfer between melanocytes and keratinocytes in the skin

Nanoemulsion is characterized as a thermodynamically unstable colloidal dispersion of two immiscible liquids. Within this emulsion, one of the liquids constitutes the dispersed phase, while

the other serves as the dispersing medium [3]. The droplets in nanoemulsion typically exhibit diameters spanning from 10 to 200 nm, and each droplet is enveloped by a protective coating of emulsifier molecules.

The Azelaic Acid nanoemulsion would typically provide context and background information to set the stage for the research. It may include the following elements:

1.1.1 Background: Briefly introduce skin hyperpigmentation disorders, emphasizing their impact on social behavior.

Highlight the challenges in treating these disorders, especially focusing on resistance to various therapeutic modalities.

1.1.2 Azelaic Acid as a Therapeutic Target: Discuss the significance of tyrosinase inhibition in melanogenesis and its role in hyperpigmentation treatment.

Introduce Azelaic Acid as an iron chelator known for its tyrosinase inhibitory properties.

1.1.3 Limitations of Azelaic Acid in Topical Administration: Address the hydrophilic nature of Azelaic Acid, which hampers effective skin penetration. Mention adverse events reported in topical administration due to this limitation.

1.1.4 Nanoemulsion as a Drug Delivery System: Provide an overview of nanoemulsion as a nanotechnology-based drug delivery system. Emphasize its potential in modulating drug permeation and enhancing efficacy, especially in addressing hydrophilic drug delivery challenges.

1.1.5 Research Objective: Clearly state the primary goal of the research, which is the creation and evaluation of an Azelaic Acid nanoemulsion for optimal skin delivery.

By incorporating these elements, the introduction sets the foundation for understanding the rationale behind developing an Azelaic Acid nanoemulsion and the potential impact it could have on addressing challenges associated with skin hyperpigmentation disorders [4].

1.2 Methodology:

1.2.1 Characterization of the Drug

Azelaic Acid was characterized for the following parameters:

1.2.1.1 Physical properties

Physical properties like appearance, color, and odour are observed to provide valuable information about the characteristics of substances. The appearance of a material helps identify its state of matter, while color is determined by how it interacts with light, aiding in substance differentiation. Odor, on the other hand, is linked to a substance's chemical composition, making it a useful identifier. The sample of Azelaic Acid powder was inspected visually to check appearance, color and odour. Physical form of Azelaic Acid is crystalline powder, white in color, odourless and molecular weight 142.12 g/mol have been reported [5].

1.2.1.2 Melting Point

Observation of the melting point is crucial for identifying substances, assessing purity, ensuring quality control, understanding thermodynamic properties, characterizing materials, and optimizing industrial processes. The melting point of the drug sample was determined by capillary glass method. The melting point of the drug was determined by taking small amount of drug in a capillary tube which was closed at one end. The capillary tube was placed in the thermionic melting point apparatus and the temperature was noted at which the drug was melted [6]. The reported melting point of the Azelaic Acid is 152 °C to 154 °C.

1.2.1.3 Solubility profile

The solubility profile of a substance refers to how much of it can dissolve in a given solvent under specific conditions, typically expressed as grams of solute per 100 grams of solvent. It aids in material identification, process optimization, and drug formulation by providing insights into how a substance interacts with different solvents.

1. Excess amount of Azelaic Acid was added to 10 ml of solvent and then allowed to dissolve for 24 hours with stirring and intermittent bath sonication.
2. The solution was then filtered by membrane filter and 1ml of filtrate was diluted with solvent and analysed spectroscopically.
3. Water, acetone, ethanol, benzene and phosphate buffer (0.2M, pH7.4) were used against as solvent to check the solubility of the Azelaic Acid.

Azelaic Acid soluble in water, ethanol, acetone; sparingly soluble in ether, and insoluble in benzene was reported.

1.2.1.4 Partition Coefficient:

The partition coefficient is the measure of the lipophilicity of a drug and an indication of its ability to cross the cell membrane. It is defined as the ratio between un-ionized drug distributed between the organic and aqueous layers at equilibrium. The partition coefficient is determined by the shake flask method using two immiscible solvents. One is aqueous phase (water), and the oil phase (n-octanol). Excess Azelaic Acid was dissolved in an equimolar mixture of n-octanol and water in a shake flask and shaken for 24 h at 25°C. The mixture was transferred to a separating funnel to separate the water and octanol phases for 48 h. The aqueous phase was then filtered, diluted, and the maximum absorbance for the drug was measured against the equivalent blanks using Shimadzu UV-1800 spectrophotometer [7]. The reported partition coefficient of Azelaic Acid.

Partition co-efficient was calculated by following formula:

$$K(o/w) = \frac{\text{concentration in organic phase}}{\text{concentration in aqueous phase}} \quad (1)$$

1.3 Analytical study:

1.3.1 By UV Spectrophotometric method

The UV spectrophotometric method is studied and developed for the quantification of Azelaic Acid in raw material using UV-Vis spectrophotometer. Among various analytical methods UV spectrophotometry is a widely utilized method in pharmaceutical analysis due to its simplicity, cost-effectiveness, and versatility. This technique is valuable for the quantitative determination of drug concentrations in formulations, providing rapid and specific results based on the characteristic UV absorption spectra of many drugs. UV spectroscopic methods for Azelaic Acid was successfully developed and validated in different solvents such as phosphate buffer 0.2M pH 7.4, water, and methanol [8,9]. UV absorption peaks of Azelaic Acid were reported at 215-216 nm and 268-269 nm in acidic or neutral solutions; 226-227nm and 309-312 nm in aAzelaic Acid line solution; 280 nm (pH of solution not reported) [Table 1].

Table 1: Reported λ_{\max} of Azelaic Acid in various solvents [165]

Sr.No.	Solvent	λ_{\max} (nm)
1.	Phosphate buffer (0.2M, pH7.4)	204
2.	Ethanol	203

1.3.2 Determination of wavelength for Maximum Absorption and preparation of calibration curves of Azelaic Acid in phosphate buffer (0.2 M pH 7.4)

A stock solution of Azelaic Acid was prepared by dissolving 2.5 mg Azelaic Acid in 50 ml phosphate buffer (0.2M, pH7.4) to obtain 50 g/ml concentration. From this stock solution, subsequent dilutions were made with phosphate buffer to obtain standard solutions containing different concentration of 2, 4, 6, 8, and 10 µg/ml. The spectrums of the standard solutions were measured using UV-Visible Spectrophotometer from 200 to 400 nm range with phosphate buffer as reference for the determination of absorption maximum (λ_{\max}). Calibration curve was prepared by measuring absorbance of above dilutions using UV-Visible Spectrophotometer at predetermined λ_{\max} (204 nm). A graph was plotted by taking concentration on X-axis and absorbance on Y-axis [10].

The calibration curve obtained from these measurements was analysed through linear regression method, in which the correlation coefficient and equation of a straight line were calculated. Buffer solution was used as reference and standard Azelaic Acid solution as control.

1.3.3 Preparation of calibration curves of Azelaic Acid in ethanol

The a forementioned procedure was used for calibration curve of Azelaic Acid in except t ethanol were used as a solvent at λ_{\max} (204 nm).

1.3.4 Drug-Excipient Compatibility

Drug and excipient compatibility study is important to ensure that the drug and the polymer are compatible with each other under test conditions before formulation preparation. To determine the drug-excipient compatibility of drug and the polymer FTIR, DSC, and XRD were performed [11].

1.3.4 Fourier Transform Infrared Spectroscopy (FTIR)

Fourier Transform Infrared Spectroscopy (FTIR) is utilized in drug-excipient compatibility studies to assess potential interactions between drugs and excipients. FTIR spectroscopy is based on the principle that different functional groups in molecules absorb infrared radiation at characteristic frequencies, producing distinct peaks in the spectrum. By analyzing molecular vibrational modes, FTIR helps identify chemical compatibility, functional groups and elucidate molecular structures in drugs, detect interaction or degradation products, and pinpoint changes in functional groups [12].

Identification of Azelaic Acid, PVA & xanthan gum mixture, and physical mixture of optimum formulation were carried out by infrared spectroscopy using Agilent Cary 630 FTIR spectrophotometer. The samples were prepared by disc method. The drug was triturated with potassium bromide (about 5mg of drug with 100 mg of dry potassium bromide) in a mortar-pestle to produce the fine and uniform mixture. The pellets were prepared by compressing the powder at 20 psi for 10 mins using potassium bromide press. Prepared sample discs were placed in the sample compartment. Samples were scanned at transmission mode in the region of 4000-400 cm^{-1} and IR spectrums were collected. The IR spectrum obtained was compared with the standard spectrum of pure drug. Reported spectrums of Azelaic Acid, PVA & xanthan gum mixture are given in the Table

5.6 to 5.8 [13].

1.3.5 Differential Scanning Calorimetry (DSC) Analysis

Differential Scanning Calorimetry (DSC) is instrumental in drug-excipient compatibility studies for determination of important thermal characteristics such as melting points and phase transitions, and facilitates the construction of phase diagrams for formulation optimization. By measuring heat flow during thermal events such as melting or decomposition, DSC helps identify potential incompatibilities and alterations in crystalline structures and ensures that the chosen excipients do not adversely affect the thermal properties of the drug during formulation [14].

Prior to heating, about 5mg of Azelaic Acid, PVA & xanthan gum mixture, physical mixtures of optimum formulation components, were placed in an aluminium pan, respectively. Then the specimens were sealed inside the pans and an empty pan was used as reference. The samples with

DSC (Q20 V24.11) method were scanned at 20 – 300 °C temperature range by calorific rate of 20 °C/min under N₂ flow. Eventually, the obtained results of the DSC thermograms were used for evaluation of drug-excipient interactions. Reported DSC thermogram of Azelaic Acid is showed at

154.34 ± 1.012 °C. The endothermic peaks of PVA shown around 210–215 °C and 225 °C [170] and the decomposition endotherm (TD) observed at 324 °C. The XG presented an endothermic peak at 178.2 °C and an exothermic peak at 283.4 °C [15].

1.3.6 X-Ray Diffraction (XRD)

X-Ray diffraction analysis (XRD) is a non-destructive technique that provides detailed information about the crystallographic structure, chemical composition, and physical properties of a material. XRD works by irradiating a material with incident X-rays and then measuring the intensities and scattering angles of the X-rays that leave the material [16, 17].

A primary use of XRD analysis is the identification of materials based on their diffraction pattern. As well as phase identification, XRD also yields information on how the actual structure deviates from the ideal one, owing to internal stresses and defects. The samples were used for XRD analysis by X-ray diffractometer. The entrapment of Azelaic Acid inside the nanoemulsion was further confirmed by the obtained diffractograms of XRD. Samples were exposed to Cu K_α radiation ($\lambda = 0.15406$ nm) that it equipped with a sample spinner operating at a current of 30 mA and a voltage of 40 kV. The measurements were performed from the initial angle $2\theta = 1^\circ$ to the final angle $2\theta = 100^\circ$. Reported XRD pattern of Azelaic Acid shown at 14.2°, 15.6857, 17.5783, 19.2°, 22.0°, 23.8135, 25.4°, 26.2619, 27.6°, 29.1017, 31.0°, 36.2°, 37.4°, 39.9° and 42.6894 for PVA shown at & for xanthan gum shown at 19.5° & 40.7° and 22.30° respectively [18, 19].

1.4 Results and Discussion

1.4.1 Characterization of the Drug

Azelaic Acid was characterized for their organoleptic properties and melting point. The obtained results of physical parameters are shown in Table 5.2.

1.4.2 Physical properties

The appearance of the sample is a white crystalline powder, odourless, colourless and molecular weight is 142.12 g/mol (Table 2). There are no changes in the observed physical properties of Azelaic Acid sample with reported one. So, we have identified and characterized the sample as Azelaic Acid [20].

Table 2: Physical properties of Azelaic Acid

Appearance	Crystalline powder
Color	White
Odor	Odorless
Molecular Weight	188.22 g/mol

1.4.3 Melting Point

Melting point of the sample obtained was 109 °C. Observed value of melting point was compared with the reported value as shown in Table 3. In this case, the observed melting point of 109 °C falls well within the reported range of 105.0 °C to 115.0 °C. This consistency between the observed value and the reported range suggests that the experimental conditions and the purity of the sample are likely suitable [21].

Table 3: Melting point of Azelaic Acid

Sample	Observed value	Reported value
Azelaic Acid	109 °C	105.0 °C - 115.0 °C

1.4.4. Solubility study of Azelaic Acid

Solubility of Azelaic Acid sample was determined quantitatively in various solvents. The solubility of Azelaic Acid sample in ethanol, phosphate buffer 7.4, acetone and benzene were found to be 39.85, 50, 43, 34 and 0.73 mg /ml respective. Soluble in water, ethanol, acetone and phosphate buffer 7.4; insoluble in benzene (Table 4). Descriptive terms can be correlated with Table 4. The concordance between the solubility of the observed sample and the reported sample in a given solvent signifies methodological consistency, sample purity, and data reliability. Matching solubility profiles also imply comparable sample purities, as impurities could influence solubility behavior.

Table 4: Classification of Solubility according to IP

Descriptive term	Approximate volume of solvent in millilitres per gram of solute
Very soluble	Less than 1
Freely soluble	From 1 to 10
Soluble	From 10 to 30
Sparingly soluble	From 30 to 100
Slightly soluble	From 100 to 1000
Very slightly soluble	From 1000 to 10,000
Insoluble or practically insoluble	More than 10,000

Table 5: Solubility profile of Azelaic Acid

Solvents	Solubility (mg/ml)	Descriptive term
Ethanol	39.85	Soluble
Water	50	Slightly soluble
Phosphate buffer 7.4	43	Soluble
Acetone	34	Soluble
Benzene	0.73	Practically insoluble

1.4.5. Partition Coefficient

As the partition coefficient value increases, the drug's ability to cross the biological cell membrane increases. Since biological membranes are lipid centric, a highly lipophilic drug molecule exhibits passive absorption and hydrophilic drug faces challenges due to its poor ability to permeate the skin.

$$\text{Log } P = \text{Log} \frac{\text{concentration in organic phase}}{\text{concentration in aqueous phase}} = \text{Log} \frac{0.92}{11} = -1.0776 \dots \dots \dots (2)$$

Log P for Azelaic Acid was found to be -1.077 indicates that it has a higher affinity for the aqueous phase (water) than the lipophilic phase (octanol). This suggests that Azelaic Acid is more liophilic in nature. The justification for this log P value could be related to the chemical structure of kojic acid, which likely contains polar functional groups, making it more soluble in water than in octanol. The observed partition coefficient of -1.077, slightly divergent from the reported value of -2.25, may be influenced by factors such as variations in experimental conditions, sample purity, precision of measurement instruments, calibration differences, solvent variability, and data reporting practices.

1.5 Analytical study

1.5.1 By UV Spectrophotometric method

1.5.2 Determination of wavelength for Maximum Absorption and preparation of calibration curves of Azelaic Acid in phosphate buffer (0.2 M pH 7.4)

In qualitative analysis of Azelaic Acid in phosphate buffer (0.2 M pH 7.4), the standard solution of Azelaic Acid with a concentration of 6 µg/ml gave a maximum wavelength at 204 nm with an absorbance of 0.332. Figure 3 illustrates the spectrum scan of AZELAIC ACID . Meanwhile, the reported Azelaic Acid spectrum in phosphate buffer (0.2 M pH 7.4) had the same maximum

wavelength at 204 nm. It shows that Azelaic Acid was positively identified in the sample by UV spectrophotometry.

The reading of the solutions was performed in UV spectrophotometer at a wavelength of 204 nm. Standard curve was plotted with concentration at x-axis and absorbance at y-axis and calculated the equation of the straight line and the linear regression coefficient. Regression equation for standard curve was $0.0515x + 0.0124$ and correlation coefficient (R^2) was found to be 0.9963 signifying that a linear relationship existed between absorbance and concentration of Azelaic Acid as shown in Figure 3 [22].

The analytical curve of AZELAIC ACID in a phosphate buffer solution was performed to analyze the results of skin permeation because the phosphate buffer solution was used as the receptor solution.

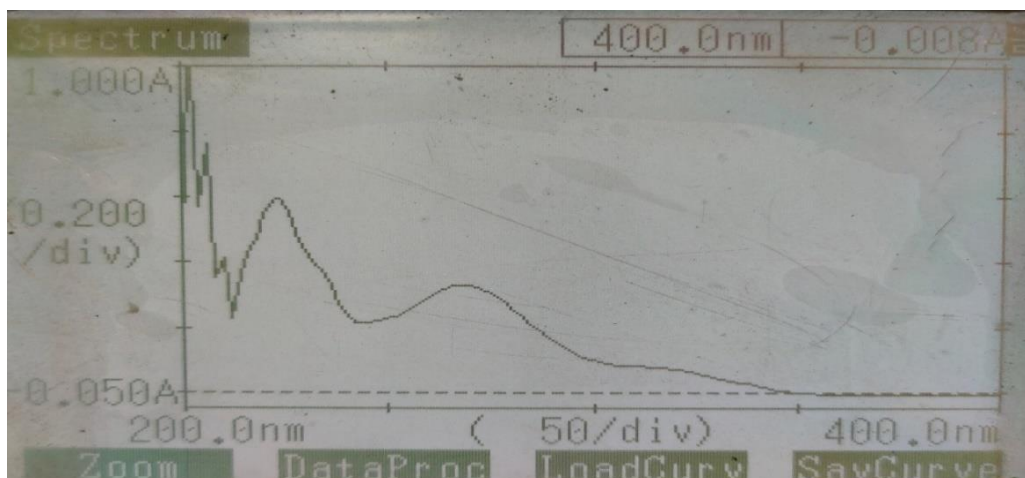


Figure 3: λ_{max} of Azelaic Acid in phosphate buffer (0.2M, pH 5.4)

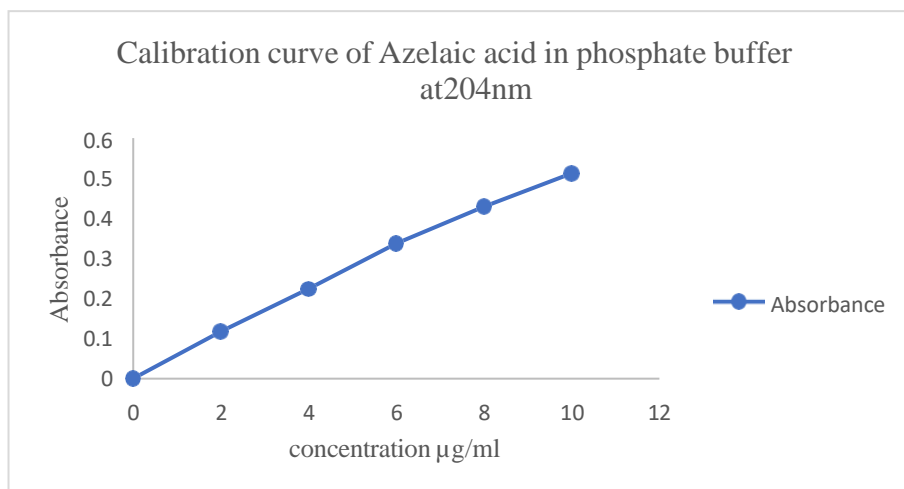


Figure 4 Calibration curve of Azelaic Acid in phosphate buffer (0.2M, pH 5.4)

1.5.3 Preparation of calibration curves of Azelaic Acid in water and methanol

A. In Water

The UV spectrum of Azelaic Acid in water showed the maximum absorption at a wavelength of 204 nm. The reading of the solutions was performed in UV spectrophotometer at a wavelength of 204 nm. Standard curve was plotted with concentration at x-axis and absorbance at y-axis and calculated the equation of the straight line and the linear regression coefficient. Regression equation for standard curve was $y = 0.038x - 0.013$ and correlation coefficient (R^2) was found to be 0.992 signifying that a linear relationship existed between absorbance and concentration of Azelaic Acid as shown in Figure 5. The analytical curve of Azelaic Acid in water was performed to use in screening study of nanoemulsion [23].

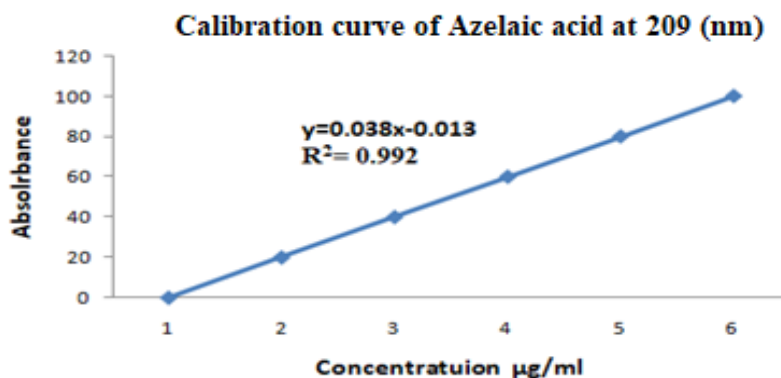


Figure 5: Calibration curve of Azelaic Acid in water

B. In Ethanol

The UV spectrum of Azelaic Acid in ethanol showed the maximum absorption at a wavelength of 2094 nm. The reading of the solutions was performed in UV spectrophotometer at a wavelength of 204 nm. Standard curve was plotted with concentration at x-axis and absorbance at y-axis and calculated the equation of the straight line and the linear regression coefficient. Regression equation for standard curve was $0.0201 - 0.0083$ and correlation coefficient (R^2) was found to be 0.9889 signifying that a linear relationship existed between absorbance and concentration of Azelaic Acid as shown in Figure 6.

The analytical curve of Azelaic Acid in methanol was performed to analysis drug content and entrapment efficiency of the Azelaic Acid and in screening study of nanoemulsion [24].

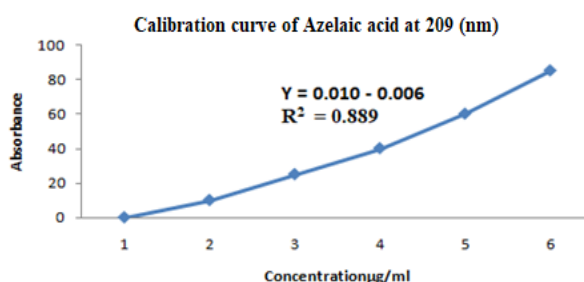


Figure 6: Calibration curve of Azelaic Acid in ethanol

1.6 Drug-Excipient Compatibility

1.6.1 Fourier Transform Infrared Spectroscopy (FTIR)

1.6.1.1 FT-IR-Azelaic Acid

The FT-IR spectral details of Azelaic Acid are given in Figure 7,8 and Table 6.



Figure 7: FTIR of the sample Azelaic Acid & the standard Azelaic Acid

Table 6: FTIR interpretation of Azelaic Acid

Characteristics Peaks	Reported (cm ⁻¹)	Observed (cm ⁻¹)
Amines N-H stretch	3281.23	3273.4
(1, 4 α -disubstituted ring)	823.48, 742.56 and 625.35	849.2, 761.0, and 653.9
the C4-C5 stretch / (deformation of-CH2)	1356	1324.6
(aliphatic- CH)	2534	2489.1
(C=C) stretching	1488, 1509	1478.1, 1516.2
(- OH)	2989.33	2975.8
alcohol	1050	1049.9
C5-O-H bending	1128	1127.0
C=O stretch	1523	1520
(C-O-C stretching)	1055	1053.7
the O1-C6 stretch	1049	1051

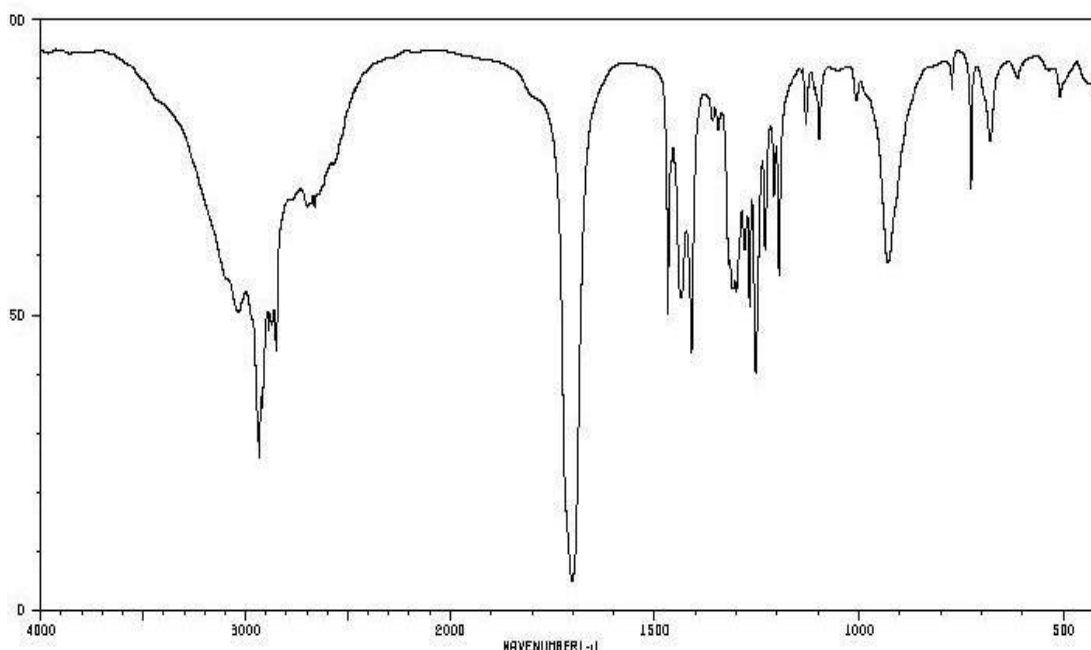


Figure 8: FTIR of Azelaic Acid

FTIR studies were performed to find out any chemical interaction between drug and formulation components during the preparation of the Azelaic Acid nanoemulsion. FTIR spectra for PVA & xanthan gum mixture, physical mixture of Azelaic Acid, PVA & xanthan, Azelaic Acid nanoemulsion and free Azelaic Acid drug are shown in Figure 8 to 10.

The FTIR spectrum of Azelaic Acid represented absorption bands at 3263 cm⁻¹ and 3145.9 cm⁻¹ due to O-H groups stretching vibrations, also peaks at 2925 cm⁻¹ and 2840.2 cm⁻¹ (aliphatic C-H stretching), 1610-1660 cm⁻¹ (C=O stretching of ring), 1579-1630 cm⁻¹ (C=C stretching), 1468.6 cm⁻¹ (deformation of-CH₂), 1069.7 cm⁻¹ (C-O stretching of ring), and 939.3 cm⁻¹, 861 cm⁻¹ and 752.9 cm⁻¹ (1, 4 α -disubstituted ring) [25].

Indicates a high degree of similarity in the chemical composition of the two substances. The alignment of peaks between a standard and a sample suggests that they share similar molecular structures or chemical bonds. This alignment serves as strong evidence that the sample (Azelaic Acid) contains the expected compound or exhibits the anticipated functional groups, affirming the identity or composition of the Azelaic Acid (standard) under investigation.

1.6.1.2. FT-IR-PVA & Xanthan Gum Mixture

The FT-IR spectral details of Azelaic Acid are given in Figure 9 and Table 7.

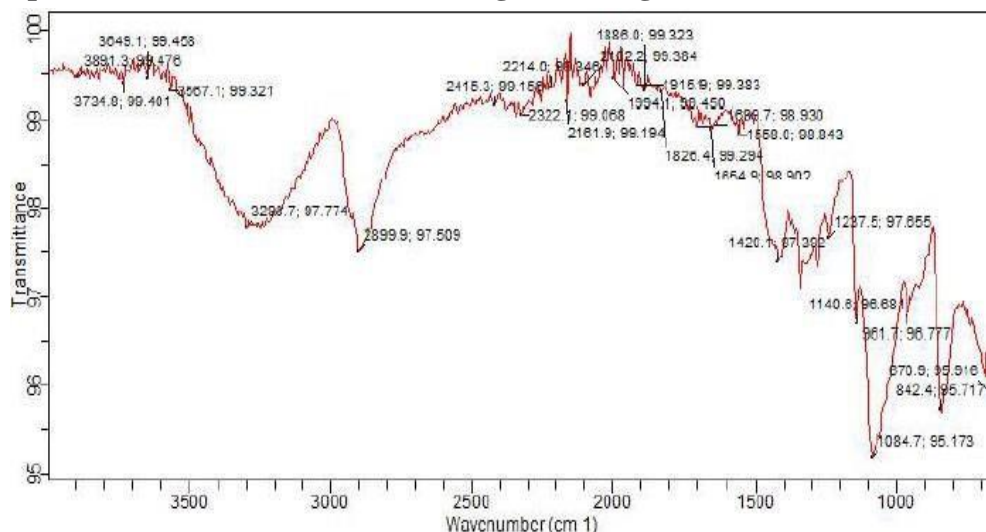


Figure 9: FTIR of PVA & Xanthan gum mixture

Table 7: FTIR interpretation of PVA

Characteristics Peaks	Reported (cm ⁻¹)	Observed (cm ⁻¹)
CH ₂ rocking	812	811.1
C–H bending vibration of CH ₂	1300–1340	1321.1
C–H broad stretching from alkyl groups	2000-2500	2325.1
nonbonded –OH stretching	3500-3650	3589.2
hydrogen bonded band	3100-3350	3230
O–H stretching arising from the intermolecular and intra-molecular hydrogen bonds	3142–3200	3189.1
shoulder stretching of C–O	1089	1098.2
C–O stretching mode	1189	1199
C=O carbonyl stretch	1591	1589
C-O stretching of acetyl groups	1060–1070	1034.1
C=C stretching vibration of PVA	1530–1561	1533.9
C–C stretching vibration	762	789.1

Table 8: FTIR interpretation of Xanthan Gum

Characteristics Peaks	Reported (cm ⁻¹)	Observed (cm ⁻¹)
axial deformation of an alcoholic (–OH) hydroxyl groups	3000–3250	3125.1
N–H stretching	3400	3409
deflection angle C–H	1330–1340	1201.1
symmetric and asymmetric stretching vibrations of the C–H group in the methyl and methylene groups	2750–2850	2823
C=O stretching of the xanthan acetate group/axial deformation of C=O of enols (β-diketones)	1430–1550	1443, 1354
C=O acetate deformation	1150	1123.1
β-glycoside linAzelaic Acid ges	600-800	688.0
axial deformation of C–O stretching (Carbonyl acetate)	1050–1200	1031.1
carboxylate asymmetric stretching	1200	1201

The FTIR spectrum of PVA & xanthan gum mixture (Figure 9) showed an absorption band at 3549.1 cm^{-1} (nonbonded $-\text{OH}$ stretching band) and 3467.1 cm^{-1} (O-H stretching vibration of the hydroxy group) of PVA, the bands at 2599.9 cm^{-1} due to asymmetric and symmetric C-H stretching vibrations of CH₂ and CH₃ groups of xanthan gum, 1389.7 cm^{-1} due to C=O carbonyl stretch of PVA, the peaks at 1468 & 1754.9 cm^{-1} both are attributed to the C=C stretching vibration of PVA and C=O stretching of the xanthan acetate group respectively, 1425 cm^{-1} due to C-H bending vibration of CH₂ of PVA, and the peak corresponding to C-O stretching occurs at approximately 1084.7 cm^{-1} . In addition, the bands were observed at the band 842 cm^{-1} due to the C-C stretching vibration of PVA and β -glycoside linAzelaic Acid ges of xanthan gum.

Based on that FT-IR spectrum of PVA & Xanthan gum functional groups, the peak accorded with reported peaks of PVA & Xanthan gum. Based on the above result the PVA & Xanthan gum mixture was confirmed as in its pure form without by-products and compatible with each other [26].

1.6.1.3. FT-IR-physical mixture of Azelaic Acid nanoemulsion

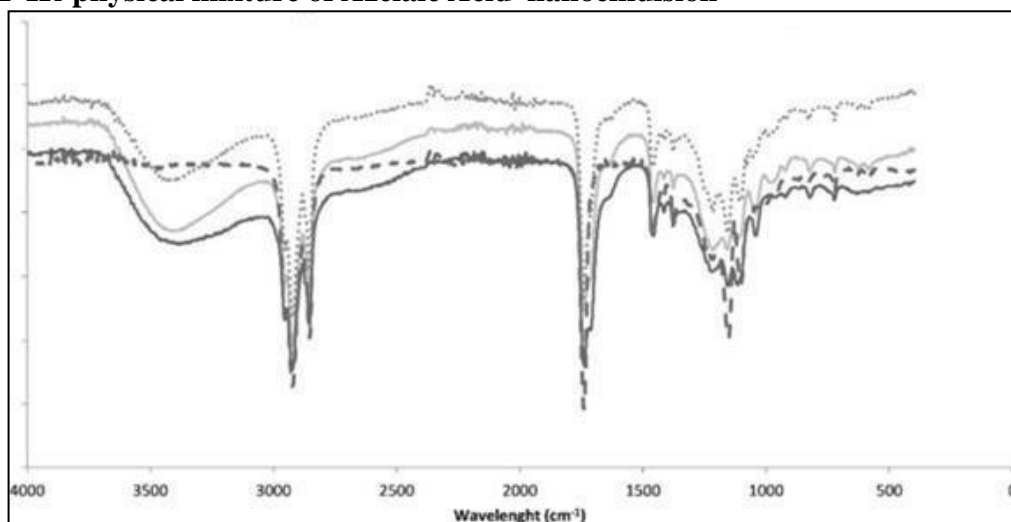


Figure 10: FTIR of physical mixture of Azelaic Acid nanoemulsion

In the FTIR spectrum of physical mixture of Azelaic Acid, characteristic peaks related to aliphatic -CH stretching, C=C stretching, stretching of (-OH) group, and C=O stretching of Azelaic Acid were still recognisable, it demonstrated that there was no shift in the characteristic peaks related to stretching vibrations of functional group of Azelaic Acid. Similarly, the characteristic absorption peaks of PVA at 1330.1 , 1030.6 , 1509.7 , and 1376.0 cm^{-1} and the characteristic absorption peaks of Xanthan gum at 1320.1 , 2807.3 , 1534.9 , 1240.6 and 761.0 cm^{-1} present in the physical mixture of Azelaic Acid, indicating there was no interaction between drug and polymer.

The FTIR spectrum of physical mixture of Azelaic Acid showed characteristic absorption bands which were comparable with absorption bands of individual sample. From the result, these prominent peaks of drug were also present in the FTIR spectra of physical mixtures of Azelaic Acid with various excipients. So, this study revealing compatibility of the selected drug with excipients [27].

1.6.1.4 Differential Scanning Calorimetry (DSC) Analysis

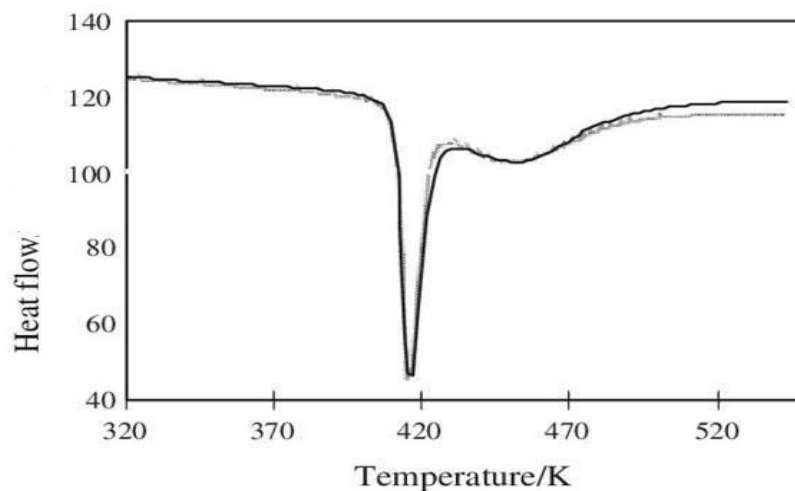


Figure 11: DSC of Azelaic Acid

The differential scanning calorimetric analysis was used for the quantitative evaluation of thermal properties of drugs and polymers such as melting point of the drug and excipients. The DSC thermograms of the Azelaic Acid sample is shown in the Figures 11. According to the DSC thermograms of Azelaic Acid sample exhibited a single sharp endothermic peak at 420 °C and this peak may be attributed to melting point, as Azelaic Acid crystallizes around this temperature. The peak of sample Azelaic Acid is similar to the reported thermo gram of Azelaic Acid . The result of the DSC analysis confirms that this sample is Azelaic Acid which is impurities free and it is extreme crystalline in nature.

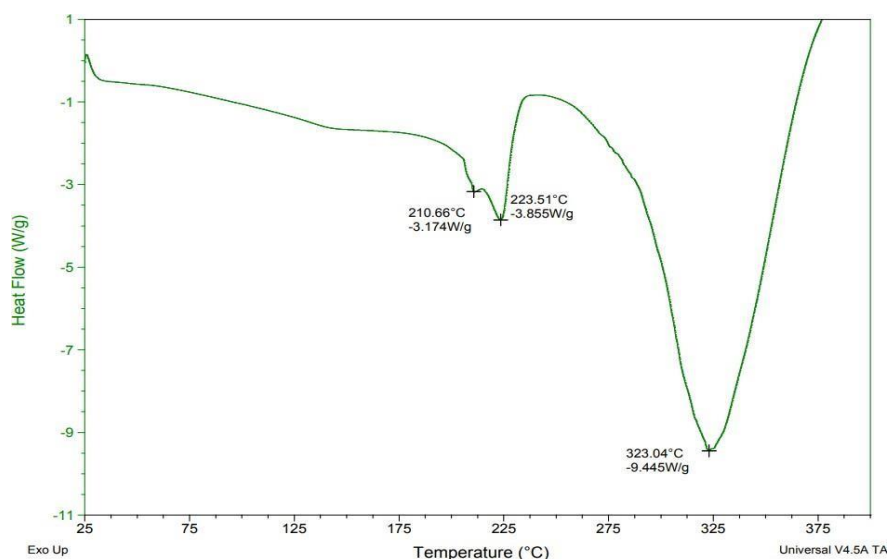


Figure 12: DSC of PVA & xanthan gum mixture

The DSC thermogram of PVA & Xanthan gum mixture is shown in the Figures 12. In this study, the DSC thermogram of PVA & Xanthan gum mixture showed three endothermic peaks. PVA showed two main transitions corresponding to melting endotherm temperature at 223.51 °C and vaporization / decomposition endotherm temperature at 324.70 °C respectively and small one at 210.66 °C and these three peaks confirm its semi-crystalline nature. The DSC thermogram of xanthan gum exhibited a melting transition slightly increased temperature at 210.66 °C which is due to peak of xanthan gum and PVA might be overlapped and indicating the semi-crystalline nature. The recorded peaks are correlated well with that reported one by other investigators for the PVA, and xanthan

gum which confirms that sample of PVA & xanthan gum mixture is identified and free from any impurities and they are compatible with each other [28].

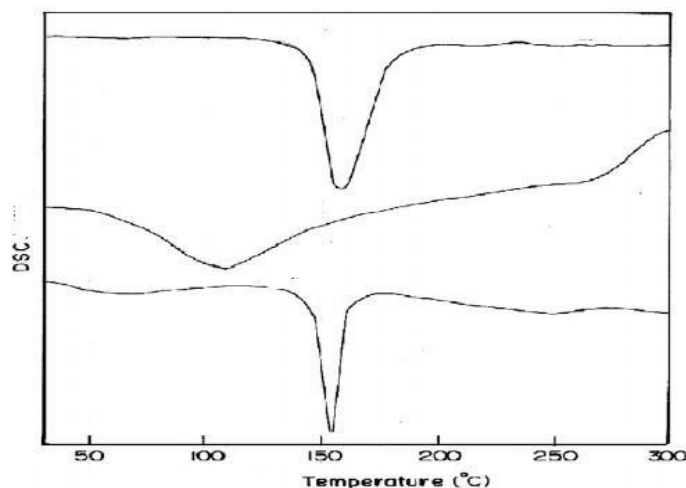


Figure 13: DSC of physical mixture of Azelaic Acid nanoemulsion

The DSC thermogram of the physical mixture of Azelaic Acid nanoemulsion is shown in the Figures

13. A thermal analysis of physical mixture has showed four DSC peaks, the first single sharp endothermic peak at 154.50 °C due to Azelaic Acid, corresponding to its melting point and indicates its crystalline nature. 2nd melting endotherm peak showed at 210.32 °C due to xanthan gum and confirmed its semi crystalline nature. The thermal behavior of PVA exhibits two characteristic endothermic peaks at 223.34 °C and 324.70 °C. These peaks correspond to the melting temperature and decomposition temperature of PVA, confirming the semi crystalline form of PVA.

It can be noticed that the DSC peaks of Azelaic Acid and PVA & xanthan gum mixture are all present and remains almost identical in the DSC thermogram of the physical mixture of Azelaic Acid, PVA & Xanthan Gum, which indicates that the physical state of Azelaic Acid, PVA & xanthan have not changed from crystalline and semi crystalline form and they are compatible with each other. On the other hand, the temperatures measured are in good agreement with values reported elsewhere [29].

1.6.1.5 X-Ray Diffraction (XRD)

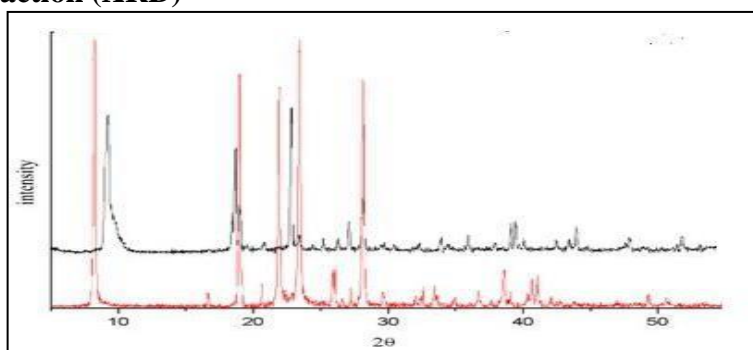


Figure 14: XRD of Azelaic Acid

X-ray diffractometry analysis was carried out to determine the nature (crystallinity or amorphous) of the sample. Figure 14 shows the XRD spectrum of the sample Azelaic Acid. It is clear that sample Azelaic Acid exhibits several sharp intense crystalline peaks. It can be observed that Azelaic Acid sample displays two intense crystalline peaks at $2\theta = 14.3132^\circ$ & 19.2311° and other significant

diffraction peaks were detected at 2θ : 21.5541°, 25.298°, 27.5791°, 30.9434°, 36.147°, 37.4011°, 39.0766°. This study indicates that observed peaks of sample Azelaic Acid are identical with the reported one and represents the crystalline nature of Azelaic Acid.

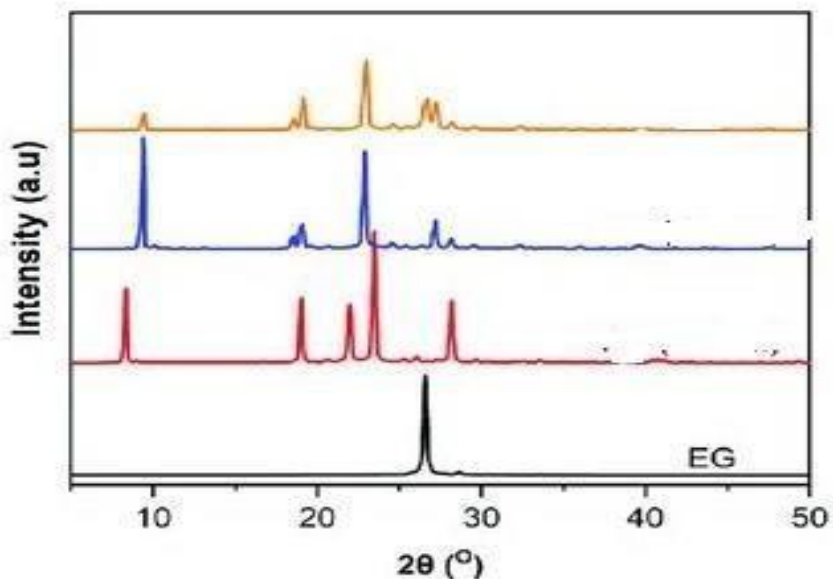


Figure 15: XRD of physical mixture of PVA & xanthan gum

XRD diffractograms of the PVA and xanthan gum mixture are shown in Figure 15. XRD spectra for PVA and xanthan gum mixture exhibited one crystalline peak of Xanthan gum at 2θ value of 22.6495° and the diffraction peak demonstrated the semi crystalline nature of it.

The XRD pattern showed a sharp diffraction peak around 19.6113° corresponding to the crystalline nature of pure PVA. The other broad peak at $2\theta = 40.6474^\circ$ can be ascribed to amorphous phases in PVA. The appearance of sharp reflections and diffuse scattering, observed from the XRD of pure PVA, is characteristic of crystalline and amorphous phases of conventional semi-crystalline polymers. So, the both peaks confirmed the semi-crystalline structure of PVA [30].

The XRD patterns of the PVA and xanthan gum mixture were accorded with the reported peaks of PVA and xanthan gum which confirms that sample of PVA & xanthan gum mixture is identified and compatible with each other.

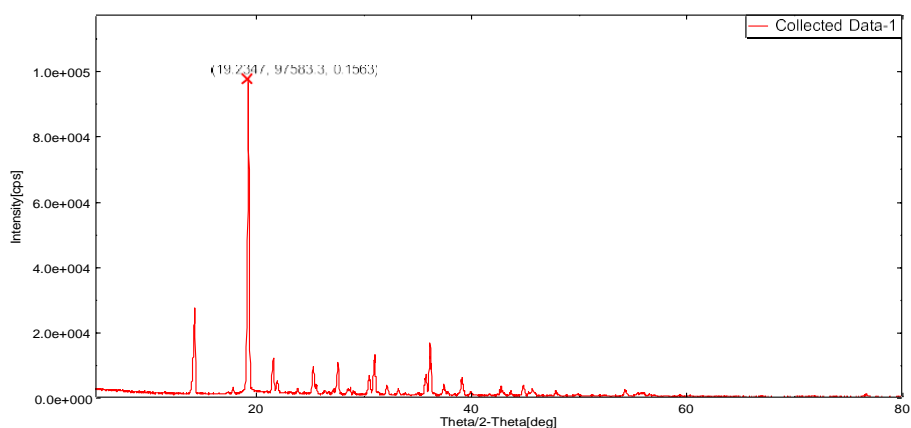


Figure 16: XRD of physical mixture of Azelaic Acid nanoemulsion

In figure 16, the XRD patterns of the physical mixture of Azelaic Acid -nanoemulsion is presented. The XRD pattern of physical mixture of Azelaic Acid -nanoemulsion exhibited the characteristic

14.2387°, 19.2234°, 21.5255°, 21.9013°, 25.2407°, 27.5741°, 30.9403°, 36.0642°, 37.3857°, 39.0068°, 39.8623°, 44.7915°.

The characteristic peak of Azelaic Acid at 2θ 19.22°, 14.2387°, 21.5255°, 25.2407°, 27.5741°, 30.9403°, 36.0642°, 37.3857°, 39.0068°, and 44.7915° have been traced and represent its crystalline nature. The characteristic peak of xanthan gum at 2θ = 21.9013° is observed and the characteristic peak of PVA at 2θ 19.22° and 39.8623° have also been traced and indicated the semi crystalline nature of xanthan gum and PVA.

The XRD patterns of physical mixture of Azelaic Acid -nanoemulsion exposed 12 the characteristic peaks of the pure Azelaic Acid and PVA & xanthan gum mixture, depicted the same peaks at the same position. Which indicates that Azelaic Acid, PVA & xanthan gum present within the physical mixture in its crystalline and semi crystalline form respectively and no phase transition has occurred in the physical mixture of Azelaic Acid -nanoemulsion and kojic acid, PVA and xanthan gum are compatible with each other.

Conclusion:

This study aimed to optimize and characterize an azelaic acid nanoemulsion for enhanced topical delivery, with a specific focus on its potential therapeutic application for skin hyperpigmentation disorders. The findings of this research contribute valuable insights into the development of a novel dermatological treatment. The optimization process, involving adjustments in formulation parameters, demonstrated its effectiveness in achieving a stable and efficient nanoemulsion system. Characterization studies provided a comprehensive understanding of the physical and chemical properties of the nanoemulsion, emphasizing its potential for practical application. The enhanced topical delivery of azelaic acid, facilitated by the nanoemulsion, holds promise for addressing skin hyperpigmentation disorders. The improved solubility and bioavailability of azelaic acid, coupled with its anti-inflammatory properties, suggest a potential therapeutic approach for conditions such as melasma and post-inflammatory hyperpigmentation. However, further studies, including in vivo experiments and clinical trials, are warranted to validate the efficacy and safety of the optimized nanoemulsion in real-world applications. Moreover, long-term stability studies and considerations for scalability in manufacturing are essential for the translation of this formulation from the laboratory to clinical practice.

References

1. Al-Edresi S, Baie S. In-vitro and in-vivo evaluation of a photo-protective kojic dipalmitate loaded into nano-creams. *Asian J Pharm Sci.* 2010;5(6):251-65.
2. Costa LC, Louchard BO, Neto EM, da Silva Giffony P, Campos FM, de Araujo TG. Development and Characterization of Azelaic Acid and Carnaúba Wax-Based Solid Lipid Microparticles. *Journal of Young Pharmacists.* 2020;12(4):309.
3. Lajis AF, Hamid M, Ahmad S, Ariff AB. Lipase-catalyzed synthesis of Azelaic Acid derivative in bioreactors and the analysis of its depigmenting and antioxidant activities. *Cosmetics.* 2017 Jul 4;4(3):22.
4. Kobayashi Y, Azelaic Acid yahara H, Tadasa K, NaAzelaic Acid mura T, TanaAzelaic Acid H. Synthesis of amino acid derivatives of Azelaic Acid and their tyrosinase inhibitory activity. *Bioscience, biotechnology, and biochemistry.* 1995 Jan 1;59(9):1745-6.
5. Norddin FA, Azhar SN, Ashari SE. Evaluation of direct esterification of fatty acid derivative of Azelaic Acid in co-solvent system: A statistical approach. *J. Biosens. Bioelectron.* 2017;8:331.
6. Xie W, Zhang J, Ma X, Yang W, Zhou Y, Tang X, Zou Y, Li H, He J, Xie S, Zhao Y. Synthesis and biological evaluation of Azelaic Acid derivatives containing 1, 2, 4-triazole as potent tyrosinase inhibitors. *Chemical Biology & Drug Design.* 2015 Nov;86(5):1087-92.
7. Noh JM, Kwak SY, Seo HS, Seo JH, Kim BG, Lee YS. Kojic acid–amino acid conjugates as tyrosinase inhibitors. *Bioorganic & medicinal chemistry letters.* 2009 Oct 1;19(19):5586-9.

8. Noh JM, Kwak SY, Kim DH, Lee YS. Kojic acid–tripeptide amide as a new tyrosinase inhibitor. *Peptide Science: Original Research on Biomolecules*. 2007;88(2):300-7.
9. Lee M, Park HY, Jung KH, Kim DH, Rho HS, Choi K. Anti-melanogenic effects of Azelaic Acid and hydroxycinnamic acid derivatives. *Biotechnology and bioprocess engineering*. 2020 Apr;25:190-6.
10. Lee YS, Park JH, Kim MH, Seo SH, Kim HJ. Synthesis of tyrosinase inhibitory Azelaic Acid derivative. *Archiv der Pharmazie: An International Journal Pharmaceutical and Medicinal Chemistry*. 2006 Mar;339(3):111-4.
11. Burnett CL, Bergfeld WF, Belsito DV, Hill RA, Klaassen CD, Liebler DC, Marks JG, Shank RC, Slaga TJ, Snyder PW, Andersen FA. Final report of the safety assessment of Azelaic Acid as used in cosmetics. *International journal of toxicology*. 2010 Nov;29(6_suppl):244S-73S.
12. Abdulbaqi MR, Rajab NA. Apixaban ultrafine O/W nano emulsion transdermal drug delivery system: formulation, in vitro and ex vivo characterization. *Syst. Rev. Pharm*. 2020 Feb 1;11:82-94.
13. O’Neil MJ, Smith A, Heckleman PE, Obenchain Jr JR, Gallipeau JR, D’Arecca MA. *Merck Index—14th Ed*. Whitehouse Station, NJ: Merck and Co. 2006:920.
14. Lewis RA. *Hawley’s condensed chemical dictionary*. John Wiley & Sons; 2016 May 31.
15. Yang Y, Engkvist O, Llinàs A, Chen H. Beyond size, ionization state, and lipophilicity: influence of molecular topology on absorption, distribution, metabolism, excretion, and toxicity for druglike compounds. *Journal of medicinal chemistry*. 2012 Apr 26;55(8):3667-77.
16. González ML, Correa MA, Chorilli M. Skin delivery of kojic acid-loaded nanotechnology-based drug delivery systems for the treatment of skin aging. *BioMed Research International*. 2013 Jan 1;2013.
17. Choi SY, Kim S, Kim H, Suk K, Hwang JS, Lee BG, Kim AJ, Kim SY. (4-Methoxybenzylidene)-(3-methoxy-phenyl)-amine, a nitrogen analog of stilbene as a potent inhibitor of melanin production. *Chemical and pharmaceutical bulletin*. 2002;50(4):450-2.
18. Kumar R, Soni GC, Prajapati SK. Formulation development and evaluation of Telmisartan Nanoemulsion. *International Journal of Research and Development in Pharmacy & Life Sciences*. 2017 Jul 15;6(4):2711-9.
19. Azelaic Acid songo WA, Pardeike J, Müller RH, Walker RB. Selection and characterization of suitable lipid excipients for use in the manufacture of didanosine-loaded solid lipid nanoparticles and nanostructured lipid carriers. *Journal of pharmaceutical sciences*. 2011 Dec 1;100(12):5185-96.
20. Khan BA, Waheed M, Hosny KM, Rizg WY, Murshid SS, Alharbi M, Khan MK. Formulation and Characterization of Carbopol-934 Based Kojic Acid-Loaded Smart Nanocrystals: A Solubility Enhancement Approach. *Polymers*. 2022 Apr 6;14(7):1489.
21. Gupta S, Pramanik AK, Azelaic Acid ilath A, Mishra T, Guha A, Nayar S, Sinha A. Composition dependent structural modulations in transparent poly (vinyl alcohol) hydrogels. *Colloids and Surfaces B: Biointerfaces*. 2009 Nov 1;74(1):186-90.
22. Gupta B, Agarwal R, Sarwar Alam M. Preparation and characterization of polyvinyl alcohol-polyethylene oxide-carboxymethyl cellulose blend membranes. *Journal of applied polymer science*. 2013 Jan 15;127(2):1301-8.
23. Devangamath SS, Lobo B, Masti SP, Narasagoudr S. Thermal, mechanical, and AC electrical studies of PVA–PEG–Ag 2 S polymer hybrid material. *Journal of Materials Science: Materials in Electronics*. 2020 Feb;31:2904-17.
24. Bernal-Chávez SA, Alcalá-Alcalá S, Tapia-Guerrero YS, Magaña JJ, Del Prado-Audelo ML, Leyva-Gómez G. Cross-linked polyvinyl alcohol-xanthan gum hydrogel fabricated by freeze/thaw technique for potential application in soft tissue engineering. *RSC advances*. 2022;12(34):21713-24.

25. Raja PB, Munusamy KR, Perumal V, Ibrahim MN. Characterization of nanomaterial used in nanobioremediation. In *Nano-bioremediation: fundamentals and applications* 2022 Jan 1 (pp. 57-83). Elsevier.
26. Kumar R, Singh A, Sharma K, Dhasmana D, Garg N, Siril PF. Preparation, characterization and in vitro cytotoxicity of Fenofibrate and Nabumetone loaded solid lipid nanoparticles. *Materials Science and Engineering: C*. 2020 Jan 1;106:110184.
27. Khezri K, Saeedi M, Morteza-Semnani K, Akbari J, Hedayatizadeh-Omran A. A promising and effective platform for delivering hydrophilic depigmenting agents in the treatment of cutaneous hyperpigmentation: Azelaic Acid nanostructured lipid carrier. *Artificial Cells, Nanomedicine, and Biotechnology*. 2021 Jan 1;49(1):38-47.
28. Khan BA, Waheed M, Hosny KM, Rizg WY, Murshid SS, Alharbi M, Khan MK. Formulation and Characterization of Carbopol-934 Based Kojic Acid-Loaded Smart Nanocrystals: A Solubility Enhancement Approach. *Polymers*. 2022 Apr 6;14(7):1489
29. Aziz SB, Abdullah OG, Hussein SA, Ahmed HM. Effect of PVA blending on structural and ion transport properties of CS: AgNt-based polymer electrolyte membrane. *Polymers*. 2017 Nov 15;9(11):622.
30. Kurnool AN, Acharya A, Ramesh B. Approaches to modify the nature of xanthan gum and characterizations to improve its functionality. *Journal of Pharmaceutical Sciences and Research*. 2019;11(1):15-20.